# Estimation of Rate-Dependent Hammerstein Model of Piezo Bender Actuator

Lenka Kuklišová Pavelková[a]
*The Czech Academy of Sciences, Institute of Information Theory and Automation*
*Pod Vodárenskou věží 4, 182 00, Prague 8, Czech Republic*

Keywords: Rate-Dependent Hysteresis, Hammerstein Model, ARX Model, Particle Swarm Optimization, Splines, Piezoceramic Actuator.

Abstract: The paper presents a Hammerstein model of a commercial piezoelectric bender PL140 from Physik Instrumente Co. The model consists of a nonlinear static part that describes the inherent hysteresis and a linear dynamic part that is represented by the auto-regressive model with exogenous input. The linear model parameters are estimated one-time using a particle swarm optimization algorithm. The rate-dependent nonlinear part is identified using input voltage data, along with a hidden variable that is obtained with the help of the inverted linear part. The experimental data are generated by a PL140 Simscape model with parameters set in accordance with catalog data.

## 1 INTRODUCTION

Piezoelectric actuators (PEAs) are essential in the field of modern science and engineering. Their high resolution and fast response distinguish them from other actuator types, such as shape-memory alloys. This makes them invaluable in a wide range of applications, including precision positioning in manufacturing, microfluidics control, medical ultrasonic therapy, and robotics (Zhou et al., 2024).

A significant challenge in PEAs is the hysteresis effect, a nonlinear relationship between input voltage and output displacement. This nonlinearity depends on input voltage amplitude and rate, causing positioning errors of 10-15% or higher at increased frequencies. It can degrade system performance and potentially lead to instability (Yuan et al., 2024).

To address the hysteresis problem, various mathematical models have been developed. These can be categorized into physics-based models and phenomenological models. Physics-based models are derived from the fundamental physical principles of the material but are often complex and not universally applicable (Yuan et al., 2024).

Phenomenological models employ mathematical representations to characterize observed hysteresis effects, often without offering a physical explanation. They can be categorized into the following methodological groups: operator-based models, differential-equation-based models, and other models. Operator-based models define hysteresis through a composition of elementary memory operators. This approach allows for high accuracy but can lead to increased computational complexity. The most popular models include Preisach model, Krasnosel'skii-Pokrovkii (KP) model, Prandtl-Ishlinskii (PI) model, and Maxwell Model (Yuan et al., 2024). Differential-equation based models describe hysteresis through differential equations that capture the memory-dependent behaviour of PEAs. The main representatives are Bouc-Wen model, Duhem model, and Dahl model (Dai et al., 2023; Yuan et al., 2024). Other methods include models such as neural networks (Son et al., 2021), Gaussian processes (Meng et al., 2022) or polynomial-based models (Yang et al., 2020).

Models can also be categorized according to whether their behavior is influenced by the rate of change of the input voltage. Rate-independent models are suitable for low-frequency inputs. They are valued for simplicity and low computational cost, though inadequate for dynamic conditions. Rate-dependent models better capture high-speed behavior. They are suitable for integration into advanced control schemes (Gan and Zhang, 2019).

The above mentioned phenomenological models are predominantly static. To capture a dynamic be-

[a] https://orcid.org/0000-0001-5290-2389



Kuklišová Pavelková, L.
Estimation of Rate-Dependent Hammerstein Model of Piezo Bender Actuator.
DOI: 10.5220/0013855300003982
Paper published under CC license (CC BY-NC-ND 4.0)
In *Proceedings of the 22nd International Conference on Informatics in Control, Automation and Robotics (ICINCO 2025) - Volume 1*, pages 532-538
ISBN: 978-989-758-770-2; ISSN: 2184-2809
Proceedings Copyright © 2025 by SCITEPRESS – Science and Technology Publications, Lda.

havior, it is convenient to use the Hammerstein model that offers a structured, phenomenological approach to modeling hysteresis by decoupling the static nonlinear hysteresis characteristics from the dynamic behavior of the system (Dai et al., 2023). This model consists of two parts connected in series: a static nonlinear component that captures the hysteresis effects and a linear dynamic block that reflects the system's dynamic response.

This method provides a significant degree of flexibility. The nonlinear block can be represented by any of the above mentioned phenomenological models making the Hammerstein model adaptable to diverse hysteresis behaviours (Dai et al., 2023).

From now on, we will focus on the Hammerstein model of a piezo actuator with a rate-dependent nonlinear static part. In this context, the static nonlinearity is usually described by the Bouc-Wen model. In (Zhang et al., 2021) and (Barbosa et al., 2020), it is coupled with auto-regressive exogenous (ARX) model, in (Liu et al., 2023), with a mass-spring-damper system and in (Yang et al., 2022), with a fractional dynamic model. Modified PI model together with online infinite impulse response is used in (Yi et al., 2022). In (Zhang et al., 2023), a static Preisach model and a dynamic transfer function are combined. In (Jin et al., 2024), Hammerstein model consists of an optimized composite neural network and an auto-regressive exogenous model in series.

Here, we will focus on a rate-dependent Hammerstein model of a specific piezo actuator, the PL140 model from Physik-Instrumente. We will build on a recently published study (Pavelková Kuklišová and Belda, 2024) that describes the mentioned piezo actuator using an Hammerstein model but does not consider rate dependency. We will extend the model applicability to rate-dependent scenarios. Our aim is to build a simple and reliable algorithm that can be easily integrated into a control system with piezoelectric actuator.

# 2 HAMMERSTEIN MODEL

This section presents a rate-dependent Hammerstein model of a piezo bender actuator a its estimation.

A discrete time Hammerstein model is a well-established framework for data-driven PEA description. It consists of a nonlinear static part serially connected with a linear dynamic part, see Figure 1. The block NLS describes the static hysteresis nonlinearity and the block LD describes the linear dynamic characteristic of the piezoelectric actuator.

In general, the linear and nonlinear parts of the

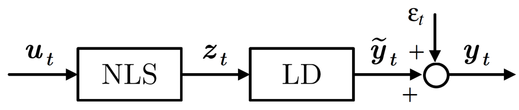


Figure 1: Block diagram of Hammerstein model – NLS corresponds to a static non-linearity, LD represents a linear dynamic behavior, $u_t$, $z_t$, $\varepsilon_t$, and $y_t$ are an input, hidden non-measurable variable, noise, and output, respectively; $t \in \{1, 2, \cdots, \bar{t}\}$ denotes a discrete time.

Hammerstein model are coupled during the identification process. However, under particular conditions, they can be identified separately (Bai, 2004). If the system is excited by an input in the form of pseudo-random binary sequences (PRBS) with sufficiently small amplitude, then non-linearity is not activated. As a result, it holds $z_t \sim u_t$. The linear part LD can therefore be identified independently.

Subsequently, after the excitation with a "rich" signal, the inverse LD model can be used to estimate the hidden variable $z_t$. Then, based on this and using knowledge of the input, it is possible to identify the NLS part.

## 2.1 Estimation of LD Part

The LD part of Hammerstein model, Figure 1, can be represented by an auto-regressive model with external input (ARX model) (Dai et al., 2023).

Here, we consider a $2^{nd}$ order ARX model, as it is an accepted method to represent electro-mechanical systems (Wilkie et al., 2002). It is defined as follows

$$y_t = \psi_t^T \theta + \varepsilon_t \tag{1}$$

where

$t \in \{1, 2, \cdots, \bar{t}\}$ denotes discrete time,

$y_t$ is an observable output,

$u_t$ is an optional known input,

$\psi_t = [y_{t-1},\ y_{t-2},\ u_t,\ u_{t-1},\ u_{t-2}]^T$ is the regression vector,

$\theta = [a_1,\ a_2,\ b_0,\ b_1,\ b_2]^T$, is the vector of unknown regression coefficients,

$T$ denotes the transposition,

$\varepsilon_t$ is a white noise, independent and identically distributed.

The least square (LS) method is typically used to estimate the ARX model (1) parameters, especially when the parameters need to be estimated recursively (Ljung, 1998). Here, we only need a one-time estimate of this model. We will use the particle swarm optimisation (PSO) method (Shi and Eberhart, 1998), which is simple to implement, flexible and more robust comparing to recursive LS (Jahandideh and Namvar, 2012).

Note that recently, the PSO method was used in the context of a Hammerstein rate-dependent dynamic hysteresis modeling to calculate the parameters of the Bouc-Wen model (Fu et al., 2024).

PSO is an algorithm that simulates social behavior, such as a flock of birds, to find optimal solutions to problems. It uses a swarm of $S$ particles, where each particle goes around a $D$-dimensional problem space and represents a potential solution. In PSO, particles adjust their positions based both on their own experience and the experience of the entire group. Each particle maintains a velocity vector $v_m$ and a position vector $x_m$, where index $m = 1, 2, \cdots, S$.

PSO estimation starts with a random initialization of vectors $v_m$ and $x_m$. In each iteration, the value of a given fitness function $f$ is used to update the best solution for each particle as well as the best solution for the whole swarm. The PSO estimation terminates when either the global optimum or the maximum number of iterations is reached.

The evolution of a velocity and a position of $m$-th particle at the $i$-th iteration is as follows:

$$\begin{aligned} v_{m,i+1} = & \; w_i v_{m,i} + c_{1,i} r_1 (p_{bm,i} - x_{m,i}) \\ & + c_{2,i} r_2 (g_{bi} - x_{m,i}) \end{aligned} \tag{2}$$

$$x_{m,i+1} = x_{m,i} + v_{m,i+1} \tag{3}$$

where $i$ means iteration, $w$ represents inertia weight, $c_1$ is a cognitive acceleration parameter, $c_2$ is a social acceleration parameter, $r_1, r_2 \in \langle 0, 1 \rangle$ are random numbers, $p_{bm,i}$ is the best location found by the $m$-th particle and $g_{bi}$ is the global best location of all the particles at the $i$-th iteration. The best locations are as follows:

$$p_{bm,i} = \begin{cases} p_{bm,i-1}, & \text{if } f(x_{m,i}) \geq f(p_{bm,i-1}) \\ x_{m,i}, & \text{if } f(x_{m,i}) < f(p_{bm,i-1}) \end{cases}$$

$$g_{bi} = \arg\min_{x_{m,i}} f(x_{m,i}), \quad 1 \leq m \leq S \tag{4}$$

The tuning parameters of PSO algorithm, i.e. $c_1$, $c_2$ and $w$ maintain the balance between global discovery and local detection. We have used the following approved setting (Fang et al., 2023; Belda and Pavelková Kuklišová, 2023) that prevent a trapping PSO in a local minima:

- time-varying acceleration coefficients

$$c_{1,i} = 2.5 - 2i/\alpha \tag{5}$$

$$c_{2,i} = 0.5 + 2i/\alpha \tag{6}$$

  where $\alpha$ denotes the total number of iterations.

- linearly decreasing inertia weights

$$w_i = w_{\max} - (w_{\max} - w_{\min})\, i/\alpha \tag{7}$$

  where $w_{\max}$ and $w_{\min}$ denote the maximal and minimal inertia weight, respectively.

The algorithmic summary of the ARX model (1) estimation using PSO is as follows:

**1)** Initialise the PSO algorithm parameters, i.e., the swarm size $S$, inertia weight $w$, acceleration coefficients $c_1$, $c_2$, maximum number of iterations $\alpha$, and maximum velocity $V_{max}$.

**2)** Set a swarm of $S$ particles of dimension $D = 5$ that corresponds to the size of $\theta$ in (1).

**3)** Initialise the position $x_{m,1}$ and velocity $v_{m,1}$, and $p_{bm,1}$ of each particle (m = 1, 2, $\cdots$ , $S$); and initialise $g_{b1}$ of the swarm.

**4)** Calculate each particle's fitness $f$ value that corresponds to the absolute prediction error

$$f = \sum_{i=1}^{N} |y(i) - \psi^T \hat{\theta}_i|$$

**5)** Update best local position $p_{bm,i}$ and global position $g_{bi}$ according to (4).

**6)** Update velocity $v_{m,i}$ (2) and position $x_{m,i}$ (3) of each particle.

**7)** If either iterations number $\alpha$ or fitness $f$ value reaches the threshold then **END**, else **GO** to the step 4).

## 2.2 Estimation of NLS Part

The NLS part of the Hammerstein model, Figure 1, can be identified with the help of a data set $u_t$ and $z_t$. Inputs $u_t$ are available. Hidden variables $z_t$ can be estimated from corresponding outputs $y_t$ by the help of the inverted LD part, i.e., ARX model (1), obtained in the previous step (Bai, 2004; Pavelková Kuklišová and Belda, 2024).

The inverted ARX model (1) with input $y_t$ and output $z_t$, neglecting the noise term, has the following form:

$$z_t = \frac{1}{b_0}\left(y_t - a_1 y_{t-1} - a_2 y_{t-2} - b_1 z_{t-1} - b_2 z_{t-2}\right) \tag{8}$$

where $a_1$, $a_2$, $b_0$, $b_1$ and $b_2$ correspond to the regression parameters of the ARX model (1).

Using an inverse model (8) and outputs $y_t$, that are obtained as responses to "rich" inputs $u_t$, i.e., inputs that sufficiently excite the hysteresis of the identified PEA, a hidden variable $z_t$ can be estimated.

Then, the NLS block of Hammerstein model, Figure 1, can be identified based on generated inputs $u_t$

together with estimated hidden variables $z_t$. The process of identifying hysteresis is as follows. We have a pair of data points [u,z] that form a hysteresis loop when graphically displayed. First, we split this loop into two parts to obtain two sets of values corresponding to two nonlinear functions, an "upper" one and a "lower" one, see an illustrative example in Fig. 2. Then, we can interpolate the points in both sets using splines (De Boor and De Boor, 1978).

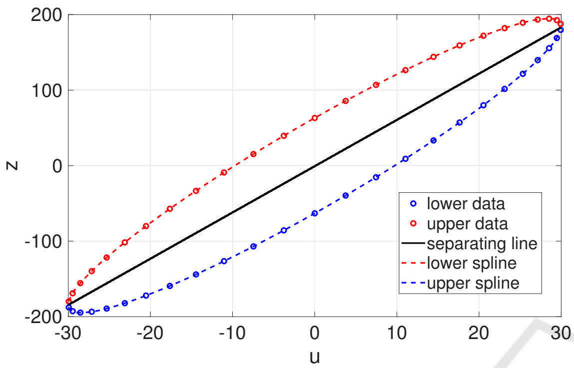


Figure 2: Data pairs $[u,z]$ for estimation of NLS block of Hammerstein model divided to the lower (blue) and upper (red) parts with separating line depicted.

Having two nonlinear functions, the identified NLS block performs as follows:

- if $u_t > u_{t-1}$, then the value $z_t$ is read from the "upper" function,
- otherwise, it is read from the "lower" function.

### 2.3 Estimation Summary

Consider the Hammerstein model of PEA in Figure 1. Then, the estimation is as follows:

**1)** Generate outputs $y_t$ by stimulating identified PEA with PRBS.

**2)** Estimate the parameters of the LD block in Hammerstein model, Fig. 1, represented by the ARX model (1) using PSO algorithm in Section 2.1 using the PRBS data.

**3)** Generate outputs $y_t$ by stimulating identified PEA with "rich" data, e.g. sin waveform.

**4)** Estimate $z_t$ in Hammerstein model, Fig. 1, according to (8) using $y_t$ from 3) as inputs.

**5)** Identify the NLS block in Hammerstein model as described in Subsection 2.2 using input data $u_t$ from 3) and output data $\hat{z}_t$ from 4)

**6)** Generate new "rich" data set as described in 3) to test the identified Hammerstein model accuracy.

## 3 EXPERIMENTS

In this section, the Hammerstein model, Figure 1, of the piezo bender actuator PL140 (Physik-Instrumente, 2025) is identified. The data for estimation are obtained using a "digital twin" of the real bender that is realized as a Simulink/Simscape model (Pavelková Kuklišová and Belda, 2024). Material constants are set according to the catalog data.

Experiments were performed for various frequencies of input signal. The sampling period was set $T_s = 5 \times 10^{-4}$ s. Note that the estimation of the LD part of Hammerstein model is rate-independent. The parameter estimation of the corresponding ARX model is therefore performed only once. The fixed inverse model is then used continuously for the calculation of a rate-dependent non-linearity.

Estimated parameters of the ARX model (1) that represents the LD part are presented in Table 2. The estimation process for 500 iterations of PSO algorithm (see Section 2.1) is shown in Figure 3.

Estimated hysteresis loops for various frequencies of input signal are depicted in Figures 4 and 5. The Figures show how the loops are split in two parts corresponding to the values of two nonlinear functions. The interpolation by splines as described in Section 2.2 is done using Matlab function *spline*.

The performance of the identified Hammerstein model was tested by a periodic step-wise signal of various frequency. The mean square error between simulated and predicted outputs for various frequencies are summarized in Table 1.

Table 1: MSE.

| $f$ (Hz) | 5 | 20 | 40 | 80 |
|---|---|---|---|---|
| MSE | 0.0129 | 0.0155 | 0.0180 | 0.0322 |

## 4 CONCLUSIONS

This paper presents an approach for modeling the rate-dependent hysteresis behavior of the piezoelectric bender actuator using a Hammerstein model structure. The main contribution is in incorporating a rate-dependent nonlinear static (NLS) block represented by two spline functions. Since the proposed model can be easily estimated, it has the potential to be used for model predictive control.

The experiments demonstrate that the Hammerstein model is suitable for capturing the hysteresis characteristics of the actuator across different input frequencies. The proposed method separates the estimation of the LD and NLS parts. The proposed model

Table 2: Estimated regression coefficients of the ARX model representing the LD part of Hammerstein model depending on the frequency $f$ of input sine signal.

| $f$ (Hz) | $a_1$ | $a_2$ | $b_0$ | $b_1$ | $b_2$ |
|---|---|---|---|---|---|
| 5 | 1.7424 | -0.9453 | 0.0012 | -0.0004 | -0.0003 |
| 50 | 1.7424 | -0.9453 | 0.0011 | -0.0004 | -0.0003 |
| 80 | 1.7424 | -0.9453 | 0.0011 | -0.0004 | -0.0003 |

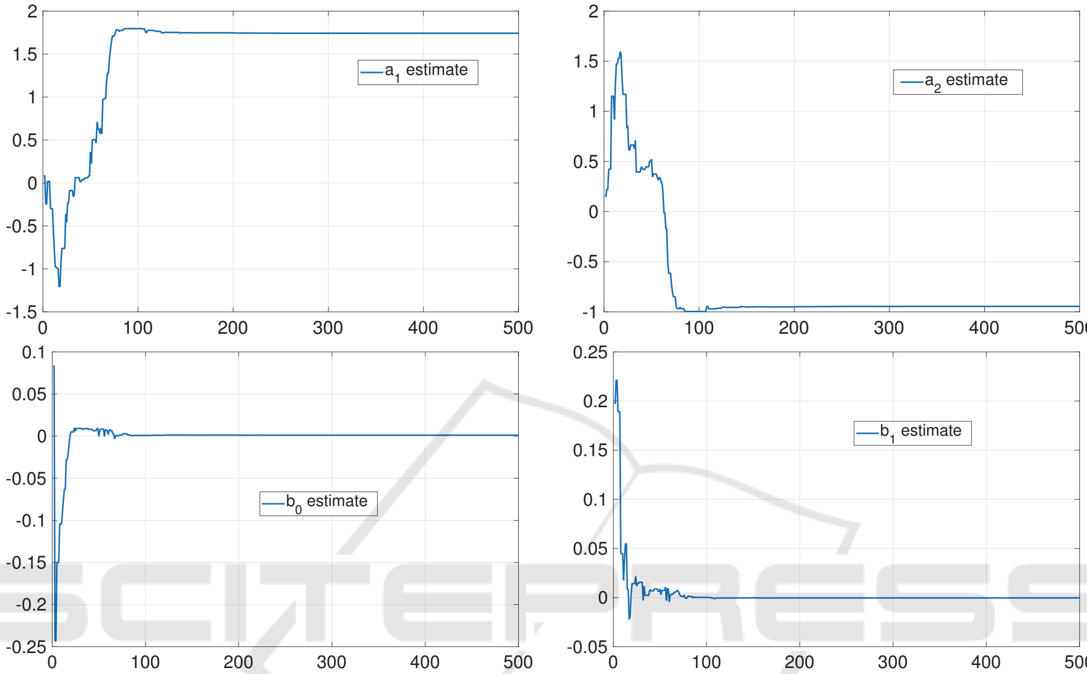


Figure 3: The courses of parameter estimation of the ARX model (1) for 500 iterations of the PSO algorithm.

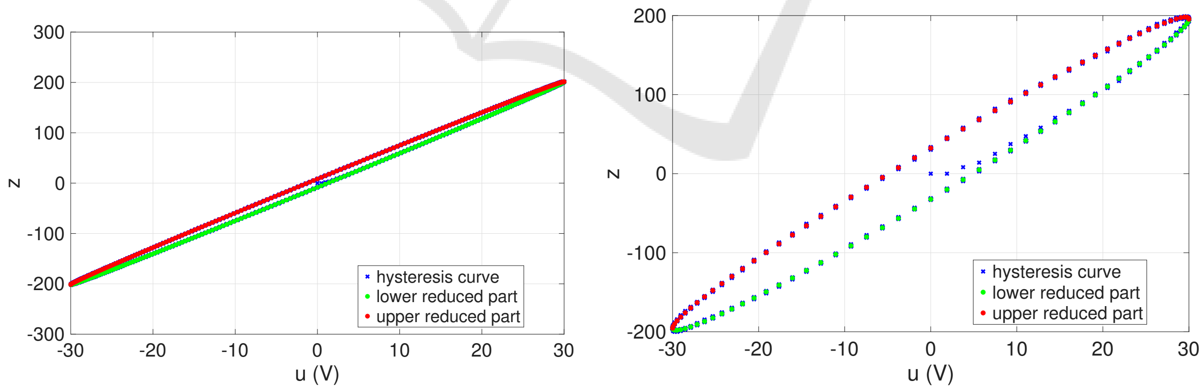


Figure 4: Hysteresis curve representing a NLS part of Hammerstein model of PL140 (blue) with indicated averaged upper (red) and lower (green) parts for $f = 5$ Hz (left) and $f = 20$ Hz (right).

yields a consistent performance across frequencies up to ca 80 Hz. For higher frequencies, the error grew rapidly. The resonance frequency of PL140 is 160 Hz. Above this frequency, the estimated hysteresis curve even became inverted. The cause may be both the simplicity of the presented model and problems related to the sampling period. This could be a topic for the further research, together with the testing on a real piezo actuator.

SCITEPRESS
SCIENCE AND TECHNOLOGY PUBLICATIONS

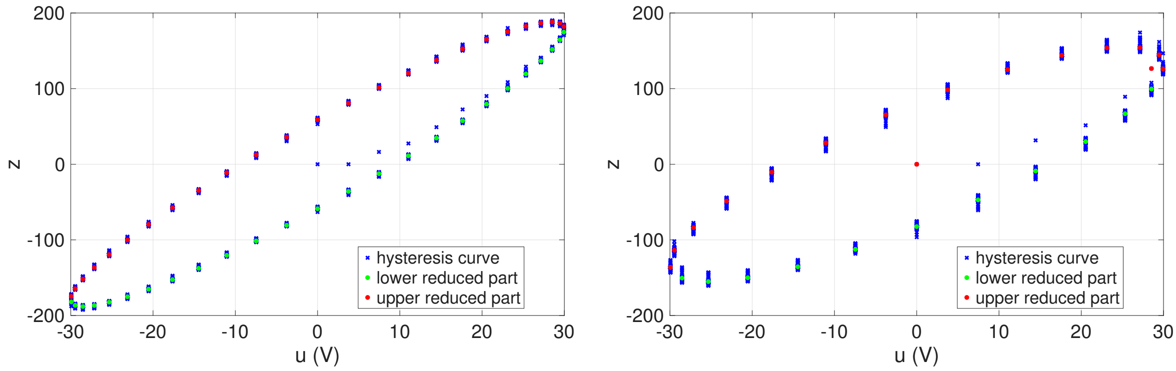


Figure 5: Hysteresis curve representing a NLS part of Hammerstein model of PL140 (blue) with indicated averaged upper (red) and lower (green) parts for $f = 40$ Hz (left) and $f = 80$ Hz (right).

## REFERENCES


Bai, E.-W. (2004). Decoupling the linear and nonlinear parts in Hammerstein model identification. *Automatica*, 40(4):671–676.

Barbosa, M. P. S., Rakotondrabe, M., and Ayala, H. V. H. (2020). Deep learning applied to data-driven dynamic characterization of hysteretic piezoelectric micromanipulators. *IFAC-PapersOnLine*, 53(2):8559–8564.

Belda, K. and Pavelková Kuklišová, L. (2023). Particle swarm optimisation for model predictive control adaptation. page 144 – 149.

Dai, Y., Li, D., and Wang, D. (2023). Review on the nonlinear modeling of hysteresis in piezoelectric ceramic actuators. *Actuators*, 12(12).

De Boor, C. and De Boor, C. (1978). *A practical guide to splines*, volume 27. springer New York.

Fang, J., Liu, W., Chen, L., Lauria, S., Miron, A., and Liu, X. (2023). A survey of algorithms, applications and trends for particle swarm optimization. *International Journal of Network Dynamics and Intelligence*, 2(1):24–50.

Fu, Y., Gao, S., Li, L., Chen, C., and Melnikau, S. (2024). Rate-dependent hysteresis modeling of piezoceramic actuators and parameter identification with an improved genetic algorithm. In *2024 9TH INTERNATIONAL CONFERENCE ON ELECTRONIC TECHNOLOGY AND INFORMATION SCIENCE, ICETIS 2024*, pages 82–86.

Gan, J. and Zhang, X. (2019). A review of nonlinear hysteresis modeling and control of piezoelectric actuators. *AIP Advances*, 9(4).

Jahandideh, H. and Namvar, M. (2012). Use of pso in parameter estimation of robot dynamics; part two: Robustness. In *2012 16th International Conference on System Theory, Control and Computing (ICSTCC)*, pages 1–6.

Jin, J., Sun, X., and Chen, Z. (2024). Inverse feedforward control of piezoelectric actuators using optimized composite neural network-based hammerstein model. *JOURNAL OF INTELLIGENT MATERIAL SYSTEMS AND STRUCTURES*, 35(20):1558–1575.

Liu, D., Dong, J., Guo, S., Tan, L., and Yu, S. (2023). Parameter identification of model for piezoelectric actuators. *Micromachines*, 14(5):1050.

Ljung, L. (1998). *System Identification: Theory for the User*. Pearson Education.

Meng, Y., Wang, X., Li, L., Huang, W., and Zhu, L. (2022). Hysteresis modeling and compensation of piezoelectric actuators using gaussian process with high-dimensional input. In *Actuators*, volume 11, page 115. MDPI.

Pavelková Kuklišová, L. and Belda, K. (2024). Identification of piezoelectric actuator using bayesian approach and neural networks. In *Proceedings of the International Conference on Informatics in Control, Automation and Robotics*, volume 1, page 591 – 599.

Physik-Instrumente, S. E. (2025). PICMA Bender PL112 - PL140 Datasheet. https://www.physikinstrumente.com/en/products/piezoelectric-transducers-actuators/pl112-pl140-picma-bender-103000. [Accessed 22-07-2025].

Shi, Y. and Eberhart, R. (1998). A modified particle swarm optimizer. In *IEEE Int. Conf. on Evolutionary Computation Proceedings. IEEE World Congress on Computational Intelligence*, pages 69–73.

Son, N. N., Van Kien, C., and Anh, H. P. (2021). Hysteresis compensation and adaptive control based evolutionary neural networks for piezoelectric actuator. *International Journal of Intelligent Systems*, 36(10):5472–5492.

Wilkie, J., Johnson, M., and Katebi, R. (2002). *Simple systems: second-order systems*, pages 173–195. Macmillan Education UK, London.

Yang, C., Verbeek, N., Xia, F., Wang, Y., and Youcef-Toumi, K. (2020). Modeling and control of piezoelectric hysteresis: A polynomial-based fractional order disturbance compensation approach. *IEEE Transactions on Industrial Electronics*, 68(4):3348–3358.

Yang, L., Zhao, Z., Zhang, Y., and Li, D. (2022). Rate-dependent modeling of piezoelectric actuators for nano manipulation based on fractional hammerstein model. *MICROMACHINES*, 13(1).

Yi, S., Zhang, Q., Xu, L., Wang, T., and Li, L. (2022).

Hysteresis online identification approach for smart material actuators with different input signals and external disturbances. *NONLINEAR DYNAMICS*, 110(3):2557–2572.

Yuan, Z., Zhou, S., Zhang, Z., Xiao, Z., Hong, C., Chen, X., Zeng, L., and Li, X. (2024). Piezo-actuated smart mechatronic systems: Nonlinear modeling, identification, and control. *MECHANICAL SYSTEMS AND SIGNAL PROCESSING*, 221.

Zhang, M., Cui, X., Xiu, Q., Zhuang, J., and Yang, X. (2023). Dynamic modeling and controlling of piezoelectric actuator using a modified preisach operator based hammerstein model. *INTERNATIONAL JOURNAL OF PRECISION ENGINEERING AND MANUFACTURING*, 24(4):537–546.

Zhang, Q., Gao, Y., Li, Q., and Yin, D. (2021). Adaptive compound control based on generalized bouc–wen inverse hysteresis modeling in piezoelectric actuators. *Review of Scientific Instruments*, 92(11).

Zhou, X., Wu, S., Wang, X., Wang, Z., Zhu, Q., Sun, J., Huang, P., Wang, X., Huang, W., and Lu, Q. (2024). Review on piezoelectric actuators: materials, classifications, applications, and recent trends. *Frontiers of Mechanical Engineering*, 19(1):6.

SCITEPRESS
SCIENCE AND TECHNOLOGY PUBLICATIONS